Molten-Salt Mediated CO_2 Capture and Utilization for Ethane Oxidative Dehydrogenation with Super-Equilibrium CO_2 Conversion

Junchen Liu, Yunfei Gao, Xijun Wang, Fanxing Li*

Abstract

CO_2-mediated oxidative dehydrogenation (CO_2-ODH) of ethane represents a promising method for carbon dioxide utilization. Existing CO_2-ODH has yet to demonstrate >50% single-pass CO yield due to the intrinsic equilibrium limitations for the CO_2-ODH reactions. We report a unique approach with mixed molten carbonates as reaction media for CO_2-ODH, which strategically partitions the CO_2-ODH reactions into gas and molten-salt phases and facilitates integrated CO_2 capture from power plant flue gases. Consequently, 89% CO yield was achieved at 770℃, doubling the equilibrium limitation. The high CO yield in turn enhances ethylene formation. Further characterizations confirm that molten-salt mediated ODH (MM-ODH) proceeds through a gas-phase cracking and molten-salt mediated reverse water-gas-shift reaction pathway. Based on this understanding, general principles to optimize the molten-salt reaction medium were developed. Thermodynamic analysis further revealed the principle for molten salt selection. Process analyses confirmed that MM-ODH has the potential to be significantly more efficient for CO_2 capture and utilization than conventional CO_2-ODH.

Introduction

With the ever-increasing global energy consumption and rising demand for the fossil energy, the annual anthropogenic CO_2 emission is projected to be 45 billion tons by 2050 under a business-as-usual scenario[1]. To avoid the dire consequences of global climate change, there is an urgent need for efficient and economically viable technologies to mitigate CO_2 emissions. Although widespread utilization of renewable energy can reduce the global carbon footprint, our continued reliance on fossil fuels calls for effective CO_2 capture, sequestration, and utilization (CCSU) technologies in the fossil energy sector.

As the first step in CCSU, CO_2 capture is the most energy intensive and is responsible for 70%~80% of the total energy consumption in carbon capture and sequestration[2–5]. Rochelle and coworkers established that 220 kWh_e of energy is required to capture and compress 1 metric ton of CO_2 from coal-fired power plant flue gas, with an estimated cost of $52/ton (2009 dollars) using the well-established solvent based technology, such as amine scrubbing[2]. Although many alternative CO_2 capture approaches have been proposed and are under different stages of research and development, significant energy consumption and cost would nevertheless incur[6–10]. The energy and cost penalties associated with CO_2 capture pose significant challenges for CO_2 utilization and sequestration since they both require a concentrated CO_2 stream. Compared to sequestration, CO_2 utilization has the potential to provide significant economic incentives by converting CO_2 into valuable products[11,12]. CO_2 utilization technologies investigated to date include CO_2 to fuel, CO_2 to chemicals, CO_2 enhanced oil recovery, etc.[11–15] Among these, CO_2-mediated oxidative dehydrogenation (CO_2-ODH) of light alkanes, particularly ethane,[14,16–24] has opened up new and exciting opportunities for: (a) producing a value-added ethylene product, which is in high demand (~200 million tons/year by 2025) and energy-intensive to produce[25]; (b) simultaneous utilization

of the abundantly available ethane resulted from the shale gas revolution[26]; (c) co-production of CO, a valuable industrial gas.

CO_2-ODH of Ethane – A Promising Approach with Intrinsic Equilibrium Limitations

Ethylene yield in commercial steam cracking processes is equilibrium limited due to the formation of H_2 as a coproduct. As such, the single-pass ethylene yield is generally limited to ~55% in steam crackers. To address this challenge, oxidative ethane dehydrogenation using CO_2 as a soft oxidant (CO_2-ODH) were widely investigated. Two primary reaction pathways for CO_2-ODH that have been reported include: (1) Direct ethane cracking reaction followed by a reverse water-gas-shift (RWGS) reaction to convert the by-product H_2 into CO and H_2O[14], as described in **Eqn. 1 and 2**; (2) Catalytic oxidative dehydrogenation of ethane with CO_2, typically on a metal oxide catalyst surface through a Mars-van Krevelen type mechanism[14]. In either reaction pathways, the overall reaction can be written as **Eqn. 3. Fig. 1** summarizes the equilibrium ethylene and CO yield in CO_2-ODH based on a C_2H_6/CO_2 = 1/1 molar-flow based feed condition. We note that byproducts such as C3+, coke, and steam reforming products are not included in the equilibrium analysis since they are kinetically limited in the context of ethane cracking conditions. This represents a commonly accepted approach to analyze ethane cracking reactions[27–31].

$$C_2H_6 \rightarrow C_2H_4 + H_2 \quad \text{(Eqn. 1)}$$

$$CO_2 + H_2 \rightarrow CO + H_2O \quad \text{(Eqn. 2)}$$

$$CO_2 + C_2H_6 \rightarrow CO + C_2H_4 + H_2O \quad \text{(Eqn. 3)}$$

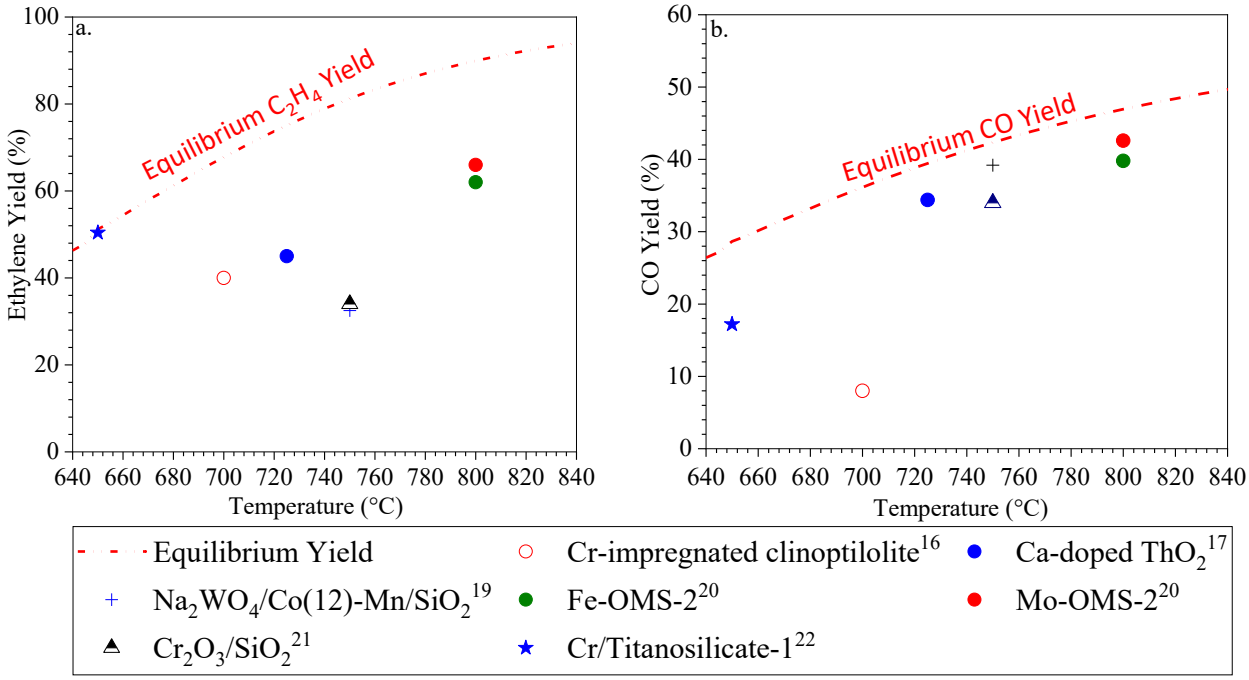

Fig. 1. Equilibrium (CO_2/C_2H_6=1) and experimentally obtained yields of selected ethane CO_2-ODH catalysts: (a) C_2H_4 yields; (b) CO yields.

To date, most CO_2-ODH studies focus on catalyst development with the goal of improving ethylene selectivity and yield. Numerous high performance catalysts have been reported along with important mechanistic insights, warranting further investigation of this important subject[13–16,18–21,23,24,32]. Although single-pass ethylene yields reported on a number of CO_2-ODH catalysts (**Fig. 1a**) were comparable to those in commercial steam ethane cracking (~55%), CO yields ($Y_{CO} = \frac{y_{CO}}{y_{CO}+y_{CO_2}}$) still remained severely equilibrium limited (**Fig. 1b**). To date, the highest CO yield reported was 55.7% at 830 ℃ for a K-Cr-Mn-O/SiO_2 catalyst.[24] However, this relatively high CO yield resulted from severe coking and dry reforming activities, which sacrificed the ethylene selectivity. Other promising CO_2-ODH catalysts include those containing Cr and/or Ni. Their CO_2 conversions are generally lower than 45%, but with satisfactory ethylene selectivity (>80%) and reasonable coke resistance[19,21,33–37]. While CO_2 conversion (or CO yield) has received little attention in most of the previous CO_2-ODH studies, it is an important parameter to consider

since: (1) Gaseous products from ethane ODH need to undergo compression and deep cooling prior to cryogenic distillation. A low CO_2 to CO conversion would significantly increase the cost and energy consumption in these stages due to the presence of H_2, negatively impacting the attractiveness of CO_2-ODH[38]; (2) the increase in the yield of CO, a high value product, can increase the overall product value while promoting the effectiveness for CO_2 utilization. Given that both RWGS and CO_2-ODH of ethane reactions are endothermic, CO_2-ODH is favored at higher temperatures from a thermodynamic standpoint. Nonetheless, the CO yield of the experimental studies reported to date are generally limited to ~45%, even when carried out at 800 C, as shown in Fig. 1. This is understandable given the intrinsic thermodynamic limitations on CO_2 conversion, which in turn limits the maximum ethylene yields. Another important challenge to conventional CO_2-ODH resides in the needs for purified CO_2, which is energy-intensive to capture and separate. To summarize, an ideal CO_2-ODH technology should be able to: (a) combine CO_2 capture and utilization into an integrated process; (b) achieve high CO and ethylene yields without being subjected to the equilibrium limitations witnessed in conventional approaches.

Integration of carbon capture and utilization has been attempted in the context of dry reforming of methane. Both Buelens et al. and Tian et al. used a hybrid system involving a calcium oxide based sorbent and Ni based catalysts to capture CO_2 followed by converting carbonate formed into CO and/or H_2[39,40]. The high operating temperature and relatively low methane feed concentration alleviate equilibrium limitations for dry (or "super dry") reforming, allowing high CO/H_2 yields. To our best knowledge, integration of CO_2 capture and utilization for ethylene production in an isothermal system have only been reported by Rezaei et al[41]. In their study, an H-Zeolite Socony Mobil 5 (H-ZSM-5) based dehydrogenation catalyst layer is used in conjunction with K_2O-CaO, Na_2O-CaO and CaO based CO_2 sorbent layer in a packed bed reactor. Captured CO_2 is released

from the sorbent by raising the reactor temperature in the ethane conversion step. 22% ethylene yield was reported, along with 14% CO_2 conversion due largely to the aforementioned equilibrium limitations. In principle, a hybrid system involving a CO_2 sorbent and heterogeneous catalyst could potentially be used for CO_2-ODH of ethane. However, more severe equilibrium limitations would be anticipated considering the high endothermicity for carbonate decomposition during the CO_2 utilization/ethane conversion step[42–44].

Herein, we proposed and demonstrated a molten-carbonate mediated ODH (MM-ODH) approach to capture and utilize CO_2 for the co-production of ethylene and CO with high yields. Strategic design of the molten-carbonate system circumvents the equilibrium limitations imposed on conventional CO_2-ODH processes, *achieving a super-equilibrium CO yield of 89.2%, doubling the equilibrium yield for conventional CO_2-ODH.* This novel process also attained 93% ethylene selectivity and 56% H_2 conversion. In the following sections, an overview of the proposed MM-ODH process and the rationale behind the equilibrium circumvention using the molten-salt as both a reaction and CO_2 capture medium are discussed first. Subsequently, the feasibility of the process is experimentally validated. An investigation of the reaction pathway is then presented as well as thermodynamic analyses to examine the selection of the molten-salt reaction media. Finally, an energy analysis is presented to determine the process efficiency for CO_2 utilization.

MM-ODH: Reaction Scheme and Proof-of-Concept

As illustrated in **Fig. 1**, CO yield with simultaneous presence of CO_2 and ethane is equilibrium limited irrespective of the ODH catalyst type. Such an equilibrium limitation would be even more severe if a solid CO_2 sorbent is used. For instance, integrating calcium carbonate as the source of CO_2 in ODH would make the CO_2-ODH process 167.6 kJ/mol more endothermic at 800℃ and limit the CO_2 conversion to 41% (vs. 47% with CO_2 co-feed) as calculated by HSC Chemistry Outotec v10. This additional thermodynamic limitation would appear to be inevitable for any CO_2-

ODH approach with integrated CO_2 capture since a system that is spontaneous for CO_2 capture would have a natural tendency to inhibit CO_2 release, adding the difficulty for CO_2 conversion in CO_2-ODH from a thermodynamic standpoint. To circumvent this challenge, we propose to use molten carbonates as a reaction medium to partition the CO_2 and ethane in the liquid phase and gas phase, respectively. Unlike solid CO_2 sorbents which have a fixed activity coefficient of 1 for the gas phase CO_2-ODH reactions, the molten carbonate system enables simultaneous equilibriums in both the gas and liquid phases, as illustrated in **Fig. 2a**. As will be further discussed through the detailed thermodynamic analyses in later sections, the eutectic formation can increase the activity of the molten carbonate salt, allowing "super-equilibrium" CO yields. A schematic of the MM-ODH approach based on the abovementioned strategy is shown in **Fig. 2b**. As illustrated, MM-ODH integrates CO_2 capture and ethane CO_2-ODH into the molten carbonate reaction medium. The MM-ODH system is operated in two cyclic steps forming a reaction loop: in Step 1, molten carbonates are converted into CO and hydroxides by H_2 generated from ethane dehydrogenation; In Step 2, the molten hydroxides subsequently capture CO_2 from a flue gas stream while regenerating the carbonates.

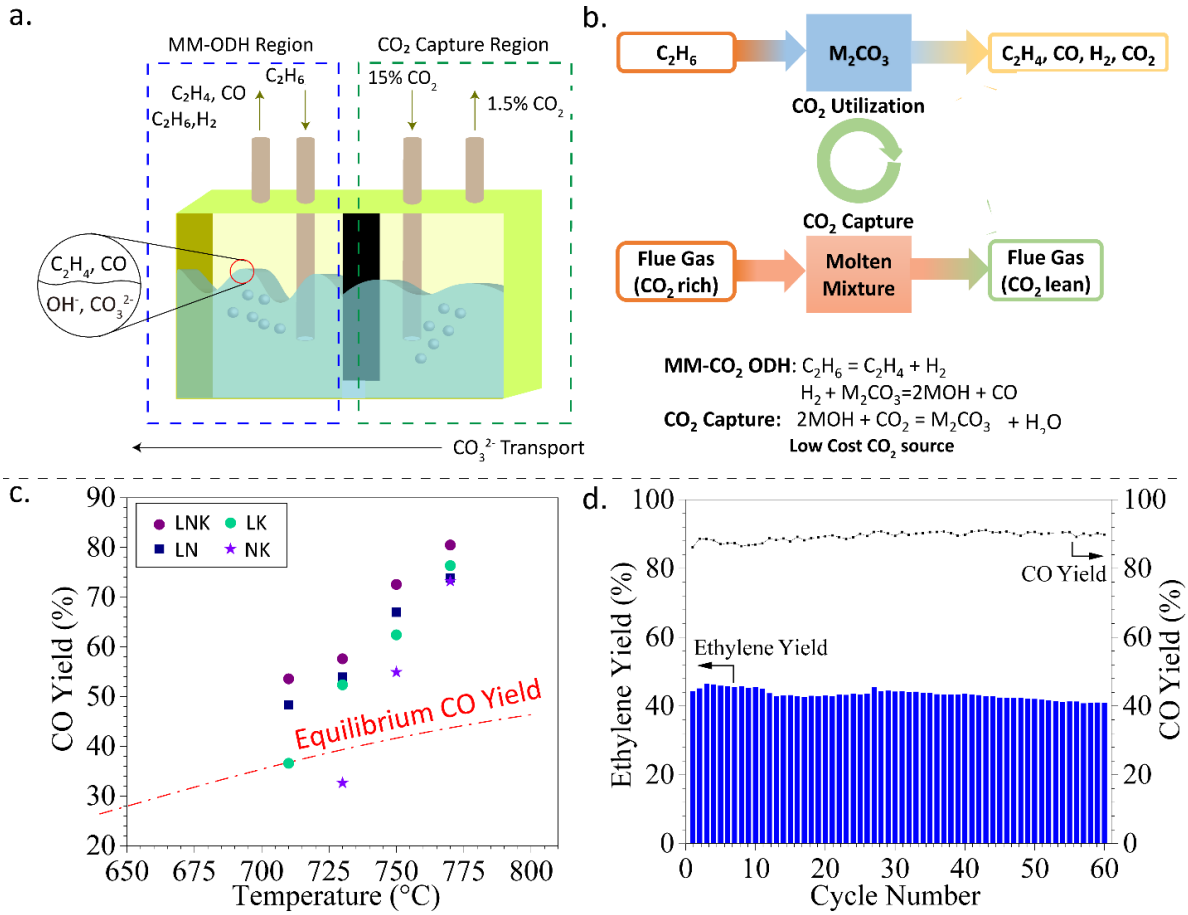

Fig. 2. (a). A conceptual reactor schematic with molten carbonate reaction media designed to simultaneously capture CO_2 and convert ethane; (b) Simplified schematic of the MM-ODH process; (c) MM-ODH reaction results for LNK, $(Li\text{-}Na)_2CO_3$ (LN), $(Li\text{-}K)_2CO_3$ (LK) and $(Na\text{-}K)_2CO_3$ (NK) at different temperatures ; (d) Performance of 60 cycle tests with LNK at 770 ℃

Fig. 2c and **2d** highlight our experimental results demonstrating the feasibility and attractiveness of MM-ODH. These results were obtained with $(Li\text{-}Na)_2CO_3$, $(Li\text{-}K)_2CO_3$, $(Na\text{-}K)_2CO_3$, and $(Li\text{-}Na\text{-}K)_2CO_3$ salt mixtures at their respective eutectic compositions and tested in an 1 inch OD alumina tube. The selection of the carbonate mixtures are based on the melting point and its stability (i.e. lower CO_2 release). $(Na\text{-}K)_2CO_3$ is not included at 710 °C due to its high melting point of 710 °C.[45] In addition, the high melting point of Li_2CO_3 (724 °C) makes it unsuitable for experimental investigation. The experimental setup and method of calculation are described in the **Fig. S1 and Table S1** (supplementary document). As can be seen in **Fig. 2c**, MM-ODH exhibited

153 significantly higher CO yields than those predicted from conventional CO_2–ODH equilibrium. For
154 all the molten salts screened, the CO yields increased with temperature. At 770℃, all molten salts
155 demonstrated CO yields ≥73%. A maximum CO yield of 89.2% was achieved with (Li-Na-K)$_2CO_3$
156 (LNK) mixed molten salts, nearly doubling the equilibrium CO yield in conventional CO_2-ODH.
157 In the extended ODH step, the CO yields could reach up to 92.2% at 770 ℃, as shown in **Fig. S2**
158 in the supplementary document. The LNK molten salts also exhibited stable ethylene yield
159 averaging at 43.4% and CO yield averaging at 89.4% for over 60 cycles (**Fig. 2d**).
160 MM-ODH also demonstrated higher ethylene yields when compared to thermal cracking. As
161 shown in **Fig. 3a** and **3b**, each molten salt eutectic system exhibited selectivity to ethylene above
162 (>90%) at 770 ℃ and ethane conversion above 70%, with a slightly higher selectivity in C_3~C_5
163 and methane than that of thermal cracking. The formation of C_{6+} species are negligible in all cases.
164 In addition, the reforming activity and coke formation are also minimal, as determined by
165 hydrogen in the supplementary documents. As one would anticipate, the ethylene selectivity
166 decreased with increasing temperature while ethane conversion and olefin yields increased.
167 Methane, C_4, and C_{6+} accounted for ≤5% of the overall product selectivity.

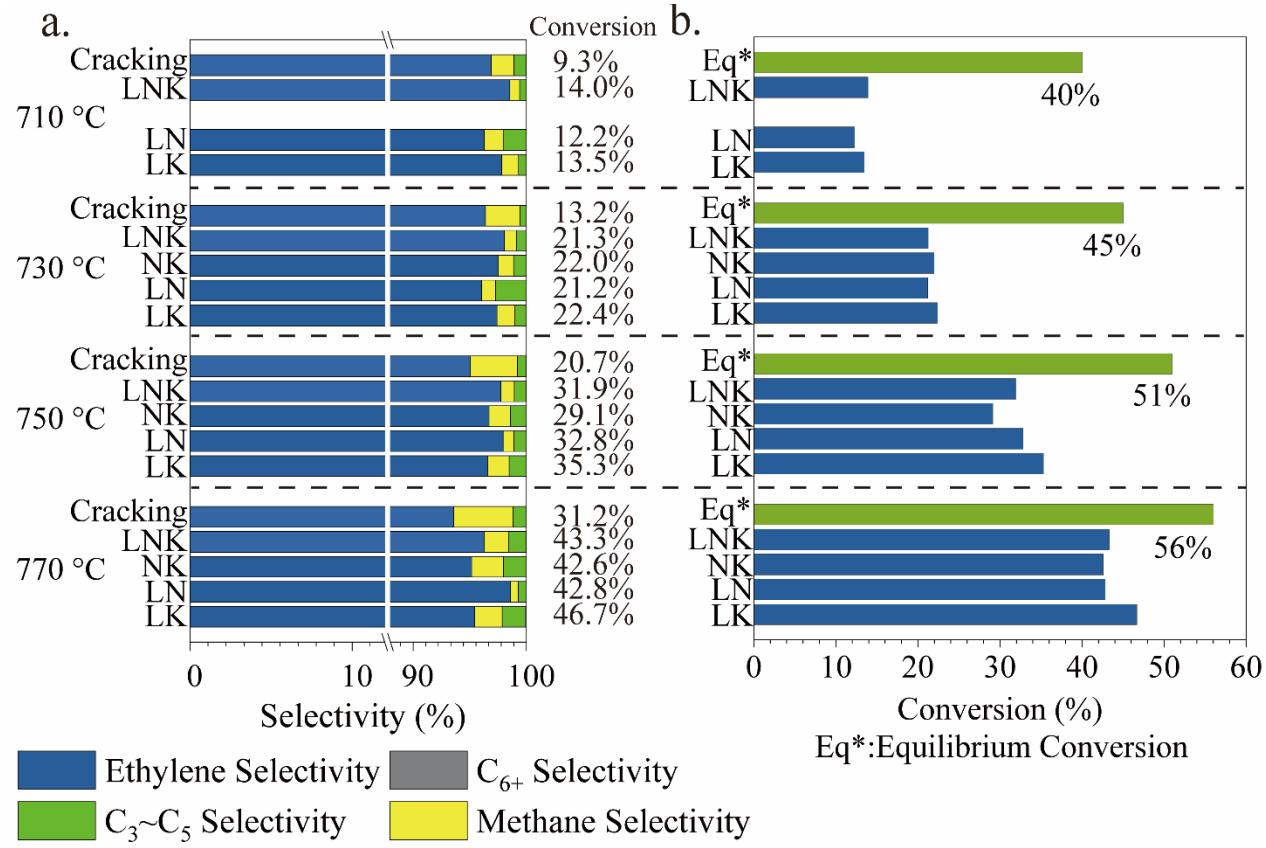

168

169 **Fig. 3.** (a). MM-ODH results with LNK, NK, LN, LK reaction media. Thermal (blank) cracking results are shown for

170 comparison purpose. Reaction conditions: 10 vol.% ethane balance Ar, 50 ml/min total gas flow rate. (b) Conversion

171 profile of the MM-ODH results in comparison with equilibrium conversion of CO_2-ODH of ethane.

172

173 The CO_2 capture and storage capability of the molten salts was further examined through

174 thermogravimetric analysis with result shown in **Figs. S3 and Fig. S4** (See supplementary

175 document). To further confirm the ability of the molten salt can capture diluted CO_2 in a flue gas

176 stream, 3 vol.% CO_2 was flown through fully decomposed Li_2CO_3, the alkali metal carbonate with

177 highest tendency to decompose into CO_2 and oxide. As shown in **Fig. S3**, the sorbent is highly

178 reactive towards this dilute CO_2 stream at CO_2 concentrations well beneath the typical flue gases

179 concentration (~12 – 15 vol.%). The CO_2 capacity of the molten salt sorbent was stable under

180 repeated cycles (**Fig. S4**). In comparison, $CaCO_3$ sorbent based CO_2 capture system tend to

experience significant sintering-induced deactivation within 20 carbonation-calcination cycles.[46–55] Although few recent studies have resulted in rather sintering resistant calcium sorbents, precise morphological controls are required.[46–55] These results demonstrate that the MM-ODH can be a promising process for CO_2 capture and utilization in the context of ethane ODH.

MM-ODH Reaction Pathway

The notably higher ethylene yields compared to thermal cracking may be explained by one of the two possible mechanisms: (a) a kinetically driven yield increase, i.e. the molten carbonate reaction medium acts as a "catalyst" to accelerate the ethane dehydrogenation reaction; or (b) a thermodynamically driven yield increase, i.e. the consumption of the H_2 through CO_2 conversion, which decreases the reverse reaction rate for MM-ODH. To probe the possible mechanism of the reactions, temperature-programmed reaction was carried out to determine the kinetic contribution, followed by *in-situ* DRIFT and H_2/CO_2 cofeed experiment to establish the roles of carbonate and hydroxide in the reaction system.

Temperature-programmed reaction (TPR) was first carried out to determine whether the molten salt would contribute to the activation of ethane. A relatively high GHSV (1200 h^{-1}) was used to ensure that the system is operated under a kinetic regime with minimal thermodynamic effects. It was determined that the onset temperature for ethane dehydrogenation was higher in the presence of the molten salt than that with ethane thermal cracking alone (**Fig. S5**). The ethylene yield in the molten carbonate system was notably lower than that of the ethane cracking in this kinetic regime, thus ruling out the catalytic effect of the molten carbonates system towards ethane conversion. The improved ethylene yields relative to thermal cracking (**Fig. 2**) are therefore thermodynamically driven due to H_2 consumption by a reverse water-gas-shift (RWGS) reaction.

To further understand the role of the molten phase in RWGS reactions, the experimental results of CO_2/H_2 cofeed in an empty tube versus H_2 feed to molten LNK were compared. The presence of

the molten salt increased CO yield by more than sixfold, from 14% to 92% (**Table S2**). The significant enhancement in the CO yield was primarily resulted from the fixation of CO_2 in the molten phase. Meanwhile, H_2 conversion was increased from 21% to 29%. These results clearly supported that the molten salt acts as a reaction medium for H_2 conversion reaction in a molten-salt mediated RWGS (MM-RWGS) reaction and it was a primary contributor to higher CO yields. These results also suggest that the "super-equilibrium" CO yield was resulted from partitioning CO_2 in the liquid phase and C_2H_6 in the gas phase. By fixating CO_2 in the molten salt, the H_2 conversion increased and the CO_2 in the product gas would be significantly lower.

The participation of the molten carbonate in the MM-RWGS reaction was further verified by *in-situ* diffuse reflectance infrared Fourier transform spectroscopy (DRIFTS) under isothermal H_2/CO_2 cycles. Due to the limitation of the instrument, the study was performed at 600℃. As shown **Fig. 4**, injection of H_2 (10%, balance Ar) resulted in a peak at 3588 cm^{-1}, assigned to the O-H stretching indicating that LiOH was formed when Li_2CO_3 was exposed to H_2, via a molten-salt mediated RWGS reaction: $Li_2CO_3 + H_2 = 2LiOH + CO$. The O-H stretching peak disappeared under 20% CO_2 and the C-O stretch peak characteristics of Li_2CO_3 appeared. This indicated that CO_2 was captured by the molten salt and LiOH was converted back to Li_2CO_3. These findings were further verified in **Fig. S6**.

To summarize, the MM-ODH reaction proceeds through a parallel gas-phase cracking and molten-salt mediated RWGS reaction pathway. That is, the presence of the molten carbonates facilitated hydrogen conversion into CO and (molten) hydroxides, which increase the ethylene yield. *In-situ* conversion of H_2 in turn enhances ethane cracking by alleviating equilibrium limitations. The alkali metal hydroxides formed in the ODH step are highly effective for CO_2 capture to regenerate

the carbonates, enabling a cyclic CO_2 capture and utilization scheme. The thermodynamic feasibility and the criteria for molten salt selection will be further discussed in the next section.

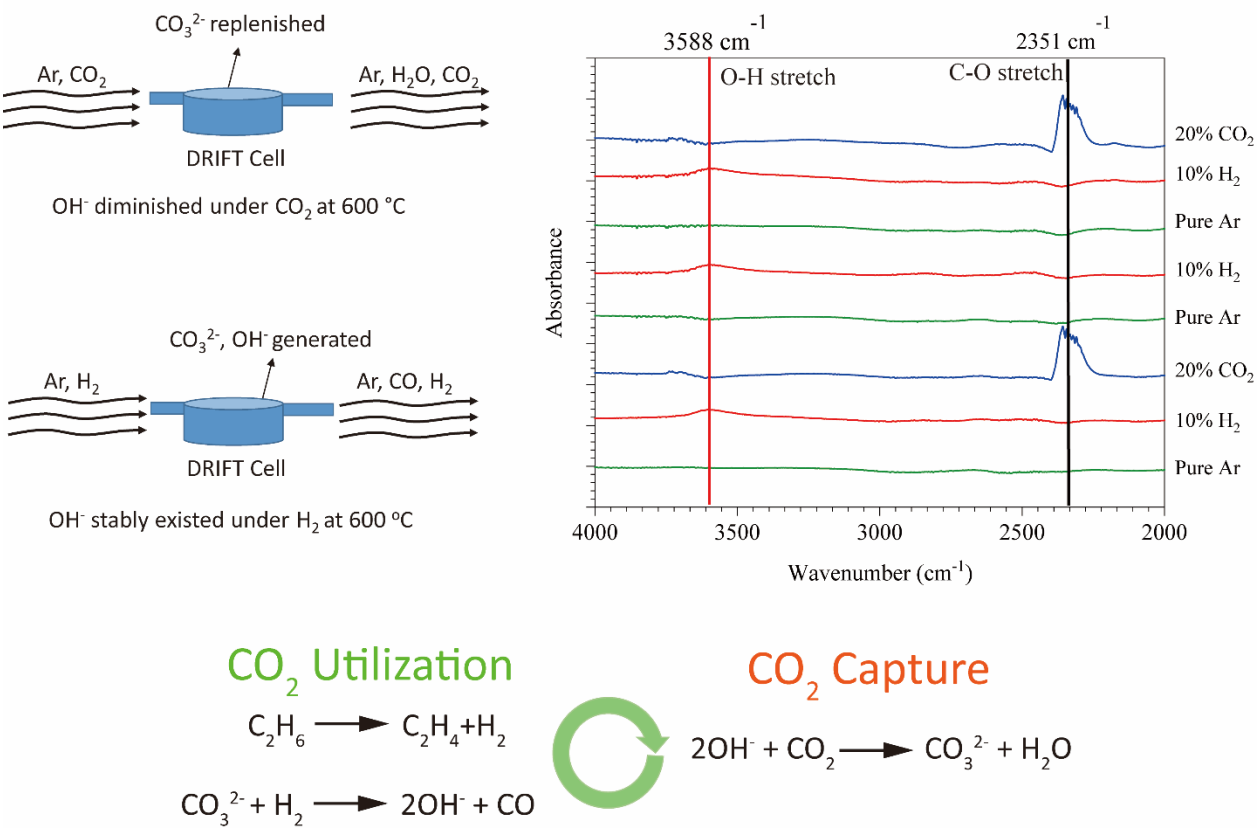

Fig. 4. *In-situ* DRIFTS experiments at 600℃ on MM-ODH reactions in the presence of a Li_2CO_3,Na_2CO_3 and K_2CO_3 eutectic reaction medium.

Thermodynamic Analysis and Effect of Molten Salt Compositions

Given that ethane conversion in MM-ODH is thermodynamically driven, and that the high CO_2 conversion was resulted from partitioning the reactions in both the gas and liquid phase, it would be informative to determine the effect of molten salt compositions on the reaction thermodynamics. Due to the complexity of the MM-ODH reaction system, a hybrid thermodynamic analysis method combining HSC Chemistry Software and numerical thermodynamic analysis was utilized. HSC Chemistry was used to establish the equilibrium among H_2, CO_3^{2-}, OH^-, H_2O, CO_2, CO, O^{2-}

between 500 to 900℃. The result was combined with the thermal cracking equilibrium constant obtained via HSC to determine the equilibrium yield of ethylene. The ethane reforming reaction, which was observed to be minimal in experiments, was not considered in the analysis.

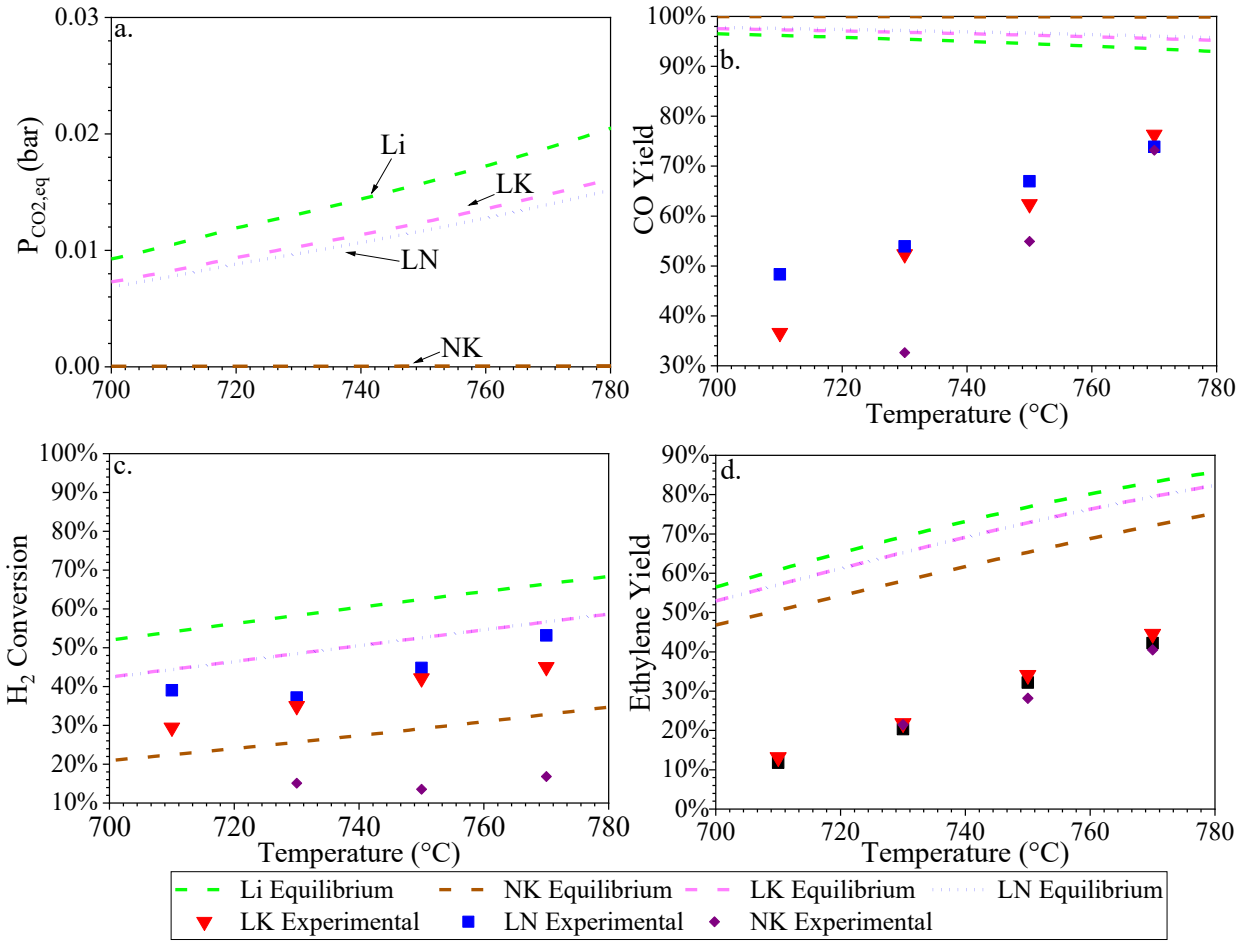

Fig. 5. (a) Equilibrium CO_2 partial pressure, (b) Equilibrium CO yield (c) Equilibrium H_2 conversion, and (d) Equilibrium ethylene yield of Li_2CO_3 (Li), 62%Li_2CO_3-38%K_2CO_3 (LK), 55%Li_2CO_3-45%Na_2CO_3 (LN), 43.5%Li_2CO_3-31.5%Na_2CO_3-25%K_2CO_3 (LNK) at the molar ratio used in experiments. The symbols correspond to the experimental results. Li_2CO_3 was not investigated experimentally due to the high melting point.

The activities of all the eutectics tested in the experiments were calculated by adopting Temkin equation to account for the deviation from the ideal solution assumption, as shown in **Equation S2-S5**. The results from these analyses, summarized in **Fig. 5**, demonstrate that the experimental

ethylene and CO yields were both below the thermodynamic limits in the two-phase system. This confirmed that while MM-ODH process circumvents the conventional CO_2-ODH equilibrium by partitioning liquid gas phase product and alternating reaction route, the reactions themselves do not violate the thermodynamic limit in the MM CO_2-ODH system.

During the ODH step, the molten salt primarily functions as a reaction medium to facilitate a modified RWGS with carbonate ions in the liquid phase. The extent of this modified RWGS reaction, which is directly related to the carbonate's tendency for decomposition, would: (i) affect H_2 conversion which in turn affects the ethylene yield by shifting the ethane pyrolysis equilibrium; (ii) affect the CO yield. **Fig. 5a** illustrates the equilibrium CO_2 partial pressures ($P_{CO_{2,eq}}$) for the carbonates of interest. Li_2CO_3, which had the greatest tendency to decompose into Li_2O and CO_2, had the highest equilibrium partial pressure. Given that Na_2CO_3 and K_2CO_3 were more stable than Li_2CO_3, mixing Li_2CO_3 with Na_2CO_3 or K_2CO_3 decreased the $P_{CO_{2,eq}}$. NK being the eutectic of Na_2CO_3 and K_2CO_3, as anticipated, has the lowest $P_{CO_{2,eq}}$. As can be expected, a low $P_{CO_{2,eq}}$ would generally lead to high CO yield (**Fig. 5a & Fig. 5b**), since minimal CO_2 would be produced during the ODH step. However, $P_{CO_{2,eq}}$ being too low would lead to low equilibrium conversion of the modified RWGS reaction and hence low H_2 conversion (**Fig. 5c**). A low H_2 conversion would in turn lead to low ethylene yield (**Fig. 5d**). An intermediate $P_{CO_{2,eq}}$ can thus enhance both CO yield (a combination of low CO_2 slippage and high carbonate conversion) and high ethylene yield. From **Fig. 5**, it can be concluded that LK provides a satisfactory balance among CO yield, H_2 conversion, and ethylene yield. LNK is not included in **Fig. 5** since the correlation for its activity coefficient is not available, but Janz et al. had shown that the $P_{CO_{2,eq}}$ of LNK was comparable to other binary eutectic, as shown in **Table S3** in the supplementary document[56]. The Gibbs free energies calculated from *ab initio* molecular dynamics (AIMD) simulations further

corroborated with this analysis, as can be seen in Fig. 6 (see Section 4 in the Supplementary information for more details). The estimated reaction Gibbs free energy (ΔG) of LK is 0.74 eV (71.40 kJ/mol) higher than that of Li_2CO_3 in terms of the modified RWGS, which would lead to a lower equilibrium conversion of modified RWGS for LK than that of Li_2CO_3. However, in terms of carbonation reaction, since the ΔG of LK is 0.78 eV (75.26 kJ/mol) lower than Li_2CO_3, the $P_{CO_{2,eq}}$ of LK would be significantly lower than that of Li_2CO_3, indicating a significantly higher CO yield. Since the ΔG of LNK on modified RWGS and carbonation reaction are in between Li_2CO_3 and LK, and that the ΔG of carbonation reaction is still negative, an intermediate equilibrium conversion of modified RWGS and a low $P_{CO_{2,eq}}$ is expected for LNK, which also exhibits its potential for desirable CO yield, H_2 conversion, and ethylene yield. Furthermore, our experiments indicated that LNK has the potential for a high H_2 conversion as shown in Table **S4** in supplementary document, supporting that this ternary eutectic could be an optimal choice for MM-ODH from a thermodynamic standpoint.

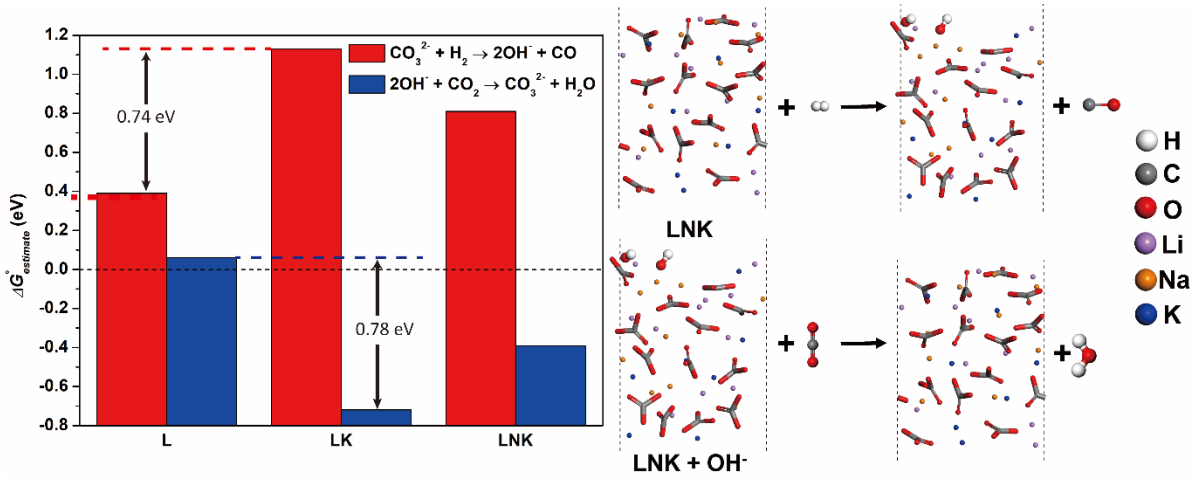

Fig 6. The *ab initio* molecular dynamic result for Gibbs free energy of modified RWGS and carbonation reaction of Li_2CO_3 (L), $(Li\text{-}K)_2CO_3$ (LK) and $(Li\text{-}Na\text{-}K)_2CO_3$ (LNK)

Energy Consumption for CO_2 Utilization

With the feasibility of MM-ODH validated by both thermodynamic analysis and experimental data, it would be desirable to compare its energy requirement when compared to the conventional CO_2-ODH. ASPEN Plus simulation was used to model the energy requirements for both MM-ODH and conventional CO_2-ODH. Both models were detailed in **Fig. S8-S10** and **Table S6-S12** in the supplementary document. For CO_2-ODH, OMS-2 catalyst was selected for modeling purpose, because it demonstrated by far the highest ethylene and CO yields based on literature report and was operated at a higher temperature than MM-ODH[20]. **Fig. 7a** demonstrated key energy requirements for the process. Unlike CO_2-ODH, the regenerator that used to capture CO_2 was a net exothermic reaction that offset 52.5% heat required from the MM-ODH reactor. The CO_2 lean stream was then used for heat integration and stream generation. Consequently, the upstream energy requirement was significantly reduced. The main energy savings in the downstream was from 91.5% lower energy requirement for amine scrubbing. Other energy saving such as lower compression and refrigeration duty was due to higher CO_2 conversion and lower moles flow on a dry basis. Energy savings were also observed from methane distillation due to 50% drop in CH_4 selectivity and CO purification due to higher H_2 conversion and minimum coking activity in the MM-ODH case. Overall, MM-ODH can lead to 31.9% energy reduction when compared to CO_2-ODH with OMS-2 in order to capture and convert 1 tonne of CO_2. We also note that both processes co-produce C_2H_4 and H_2 along with CO. In order to more accurately quantify the energy consumed for CO_2 capture and conversion (to CO), the energy associated with ethylene and H_2 production are subtracted from the overall process energy consumption, as illustrated in **Fig. 7b**. Corresponding assumptions and calculations are given in the supplementary document[38,57]. As can be seen, the energy consumption for CO_2 capture and utilization was **8.8 GJ/ton CO_2** for MM-

ODH and **15.9 GJ/ton CO_2** for CO_2-ODH with OMS-2. This corresponds to a 44.6% energy reduction from the proposed MM-ODH approach.

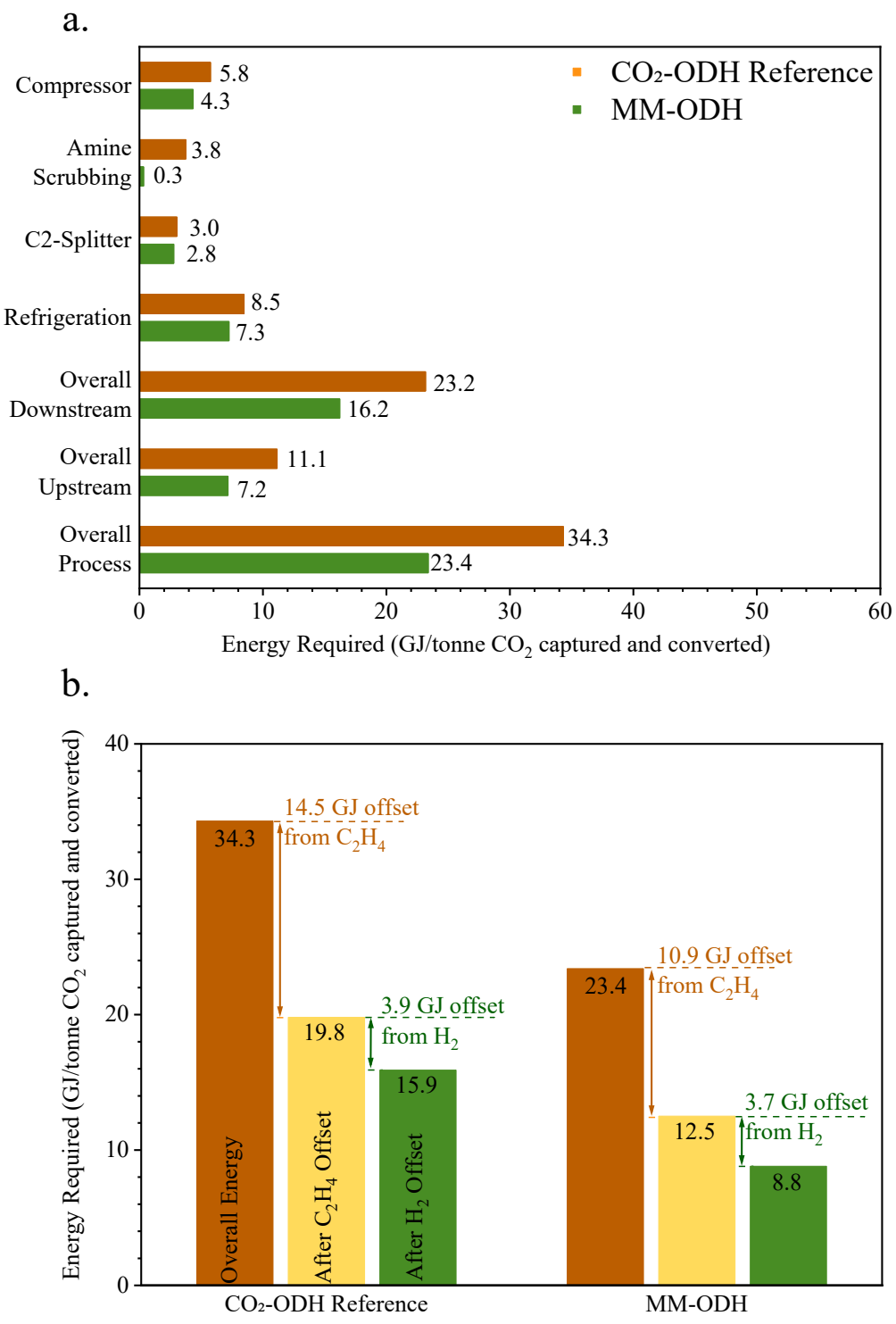

Fig. 7. (a).Energy consumptions for MM-ODH and conventional CO_2-ODH, normalized to per metric ton of CO_2 captured and converted[20]; (b) Process energy requirement for CO_2-ODH with OMS-2 and MM-ODH. The energy requirement for C_2H_4 production and H_2 production were assumed to be 9.9 GJ/ton C_2H_4 (based on stream cracking)[38] and 100 GJ/ton H_2 (based on steam methane reforming)[57].

Conclusion

The current study reports alkali metal carbonates as effective reaction media for CO_2-ODH of ethane with integrated CO_2 capture. This molten-salt mediated ODH (MM-ODH) process demonstrated a CO yield up to 89.2%, nearly doubling the equilibrium CO yield in conventional CO_2-ODH processes. In addition, an equilibrium-enhanced ethylene yield with >90% selectivity was demonstrated. The "super-equilibrium" CO yield was achieved by partitioning the CO_2-ODH reactions into both the gas and molten-salt phases, as confirmed by a detailed thermodynamic analysis. The analysis was also shown to be effective to project the relative performance of the various molten salt reaction media. Characterizations of the MM-ODH reactions indicated that ethane conversion in the presence of molten carbonate reaction media proceeds through a parallel gas-phase cracking and molten-salt mediated RWGS reaction. The presence of the molten carbonates facilitates hydrogen conversion into CO and molten hydroxides via a molten-salt mediated reverse water-gas-shift reaction (MM-RWGS). *In-situ* conversion of H_2 in turn enhanced ethane cracking by alleviating equilibrium limitations. The alkali metal hydroxides formed in the ODH step are highly effective for CO_2 capture to regenerate the carbonates, enabling stable performance for cyclic CO_2 capture followed with CO_2 utilization via ethane ODH. ASPEN Plus simulation indicates that the MM-ODH approach can result in up to 44.6% energy savings for integrated CO_2 capture and utilization.

References

1. EIA projects global energy-related CO2 emissions will increase through 2050. *IEA* https://www.eia.gov/todayinenergy/detail.php?id=41493 (2019).
2. Rochelle, G. T. Amine Scrubbing for CO2 Capture. *Science* **325**, 1652–1654 (2009).
3. Vitillo, J. G., Smit, B. & Gagliardi, L. Introduction: Carbon Capture and Separation. *Chem. Rev.* **117**, 9521–9523 (2017).
4. Liang, L. *et al.* Carbon dioxide capture and conversion by an acid-base resistant metal-organic framework. *Nat Commun* **8**, 1233 (2017).
5. Leung, D. Y. C., Caramanna, G. & Maroto-Valer, M. M. An overview of current status of carbon dioxide capture and storage technologies. *Renewable and Sustainable Energy Reviews* **39**, 426–443 (2014).
6. Zhang, X. *et al.* Post-combustion carbon capture technologies: Energetic analysis and life cycle assessment. *International Journal of Greenhouse Gas Control* **27**, 289–298 (2014).
7. Raynal, L. *et al.* The DMX™ process: An original solution for lowering the cost of post-combustion carbon capture. *Energy Procedia* **4**, 779–786 (2011).
8. Pirngruber, G. D., Guillou, F., Gomez, A. & Clausse, M. A theoretical analysis of the energy consumption of post-combustion CO2 capture processes by temperature swing adsorption using solid sorbents. *International Journal of Greenhouse Gas Control* **14**, 74–83 (2013).
9. Bounaceur, R., Lape, N., Roizard, D., Vallieres, C. & Favre, E. Membrane processes for post-combustion carbon dioxide capture: A parametric study. *Energy* **31**, 2556–2570 (2006).
10. Erlach, B., Schmidt, M. & Tsatsaronis, G. Comparison of carbon capture IGCC with pre-combustion decarbonisation and with chemical-looping combustion. *Energy* **36**, 3804–3815 (2011).
11. Hepburn, C. *et al.* The technological and economic prospects for CO2 utilization and removal. *Nature* **575**, 87–97 (2019).

12. Zimmermann, A. W. *et al.* Techno-Economic Assessment Guidelines for CO2 Utilization. *Front. Energy Res.* **8**, 5 (2020).
13. Yaashikaa, P. R., Senthil Kumar, P., Varjani, S. J. & Saravanan, A. A review on photochemical, biochemical and electrochemical transformation of CO2 into value-added products. *Journal of CO2 Utilization* **33**, 131–147 (2019).
14. Gomez, E., Yan, B., Kattel, S. & Chen, J. G. Carbon dioxide reduction in tandem with light-alkane dehydrogenation. *Nat Rev Chem* **3**, 638–649 (2019).
15. Kuuskraa, V. A., Godec, M. L. & Dipietro, P. CO2 Utilization from "Next Generation" CO2 Enhanced Oil Recovery Technology. *Energy Procedia* **37**, 6854–6866 (2013).
16. Rahmani, F., Haghighi, M. & Amini, M. The beneficial utilization of natural zeolite in preparation of Cr/clinoptilolite nanocatalyst used in CO2-oxidative dehydrogenation of ethane to ethylene. *Journal of Industrial and Engineering Chemistry* **31**, 142–155 (2015).
17. Baidya, T., van Vegten, N. & Baiker, A. Selective Conversion of Ethane to Ethene via Oxidative Dehydrogenation Over Ca-doped ThO2 Using CO2 as Oxidant. *Top Catal* **54**, 881–887 (2011).
18. Valenzuela, R. X., Bueno, G., Cortés Corberán, V., Xu, Y. & Chen, C. Selective oxidehydrogenation of ethane with CO2 over CeO2-based catalysts. *Catalysis Today* **61**, 43–48 (2000).
19. Zhu, J. *et al.* Na2WO4/Mn/SiO2 catalyst for oxidative dehydrogenation of ethane using CO2 as oxidant. *Catalysis Today* **148**, 310–315 (2009).
20. Jin, L. *et al.* Studies on Dehydrogenation of Ethane in the Presence of CO_2 over Octahedral Molecular Sieve (OMS-2) Catalysts. *ChemCatChem* **1**, 441–444 (2009).
21. Wang, S., Murata, K., Hayakawa, T., Hamakawa, S. & Suzuki, K. Oxidative dehydrogenation of ethane by carbon dioxide over sulfate-modified Cr2O3/SiO2 catalysts. *Catalysis Letters* **63**, 59–64 (1999).
22. Zhao, X. & Wang, X. Oxidative dehydrogenation of ethane to ethylene by carbon dioxide over Cr/TS-1 catalysts. *Catalysis Communications* **7**, 633–638 (2006).

23. Gaab, S., Machli, M., Find, J., Grasselli, R. K. & Lercher, J. A. Oxidative dehydrogenation of ethane over novel Li/Dy/Mg mixed oxides: structure–activity study. *Topics in Catalysis* **23**, 151–158 (2008).
24. Krylov, O. V., Mamedov, A. Kh. & Mirzabekova, S. R. The regularities in the interaction of alkanes with CO2 on oxide catalysts. *Catalysis Today* **24**, 371–375 (1995).
25. Wood Mackenzie. Ethylene Global Supply Demand Analytics Service. *Ethylene Global Supply Demand Analytics Service* https://www.woodmac.com/news/editorial/ethylene-global-supply-demand-analytics-service/ (2018).
26. Oglend, A., Lindbäck, M. E. & Osmundsen, P. Shale Gas and the Relationship between the U.S. Natural Gas, Liquefied Petroleum Gases and Oil Markets. *SSRN Journal* (2013) doi:10.2139/ssrn.2295604.
27. Ranjan, P., Kannan, P., Al Shoaibi, A. & Srinivasakannan, C. Modeling of Ethane Thermal Cracking Kinetics in a Pyrocracker. *Chem. Eng. Technol.* **35**, 1093–1097 (2012).
28. Sundaram, K. M. & Froment, G. F. Modeling of thermal cracking kinetics—I. *Chemical Engineering Science* **32**, 601–608 (1977).
29. Sundaram, K. M., Van Damme, P. S. & Froment, G. F. Coke deposition in the thermal cracking of ethane. *AIChE J.* **27**, 946–951 (1981).
30. Van Geem, K. M. *et al.* Automatic reaction network generation using RMG for steam cracking of n-hexane. *AIChE J.* **52**, 718–730 (2006).
31. Venkataraman, K., Redenius, J. M. & Schmidt, L. D. Millisecond catalytic wall reactors: dehydrogenation of ethane. *Chemical Engineering Science* **57**, 2335–2343 (2002).
32. Deng, S., Li, H., Li, S. & Zhang, Y. Activity and characterization of modified Cr2O3/ZrO2 nano-composite catalysts for oxidative dehydrogenation of ethane to ethylene with CO2. *Journal of Molecular Catalysis A: Chemical* **268**, 169–175 (2007).
33. Zhang, X., Ye, Q., Xu, B. & He, D. Oxidative dehydrogenation of ethane over Co–BaCO3 catalysts using CO2 as oxidant: effects of Co promoter. *Catal Lett* **117**, 140–145 (2007).

34. Yan, B., Yao, S. & Chen, J. G. Effect of Oxide Support on Catalytic Performance of FeNi‐based Catalysts for CO_2‐assisted Oxidative Dehydrogenation of Ethane. *ChemCatChem* **12**, 494–503 (2020).
35. Yan, B. *et al.* Active sites for tandem reactions of CO_2 reduction and ethane dehydrogenation. *Proc Natl Acad Sci USA* **115**, 8278–8283 (2018).
36. Porosoff, M. D. *et al.* Identifying Different Types of Catalysts for CO_2 Reduction by Ethane through Dry Reforming and Oxidative Dehydrogenation. *Angew. Chem.* **127**, 15721–15725 (2015).
37. Yao, S. *et al.* Combining CO2 Reduction with Ethane Oxidative Dehydrogenation by Oxygen-Modification of Molybdenum Carbide. *ACS Catal.* 8 (2018).
38. Haribal, V. P., Neal, L. M. & Li, F. Oxidative dehydrogenation of ethane under a cyclic redox scheme – Process simulations and analysis. *Energy* **119**, 1024–1035 (2017).
39. Tian, S., Yan, F., Zhang, Z. & Jiang, J. Calcium-looping reforming of methane realizes in situ CO_2 utilization with improved energy efficiency. *Sci. Adv.* **5**, eaav5077 (2019).
40. Buelens, L. C., Galvita, V. V., Poelman, H., Detavernier, C. & Marin, G. B. Super-dry reforming of methane intensifies CO2 utilization via Le Chateliers principle. *Science* **354**, 449–452 (2016).
41. Al-Mamoori, A., Lawson, S., Rownaghi, A. A. & Rezaei, F. Oxidative dehydrogenation of ethane to ethylene in an integrated CO2 capture-utilization process. *Applied Catalysis B: Environmental* **278**, 119329 (2020).
42. Bui, M. *et al.* Carbon capture and storage (CCS): the way forward. *Energy Environ. Sci.* **11**, 1062–1176 (2018).
43. Gupta, H., Lyer, M. V., Sakadjian, B. B. & Fan, L.-S. Reactive separation of CO2 using pressure pelletised limestone. *International Journal of Environmental Technology and Management* **4**, (2004).
44. Sakadjian, B. B., Iyer, M. V., Gupta, H. & Fan, L.-S. Kinetics and Structural Characterization of Calcium-Based Sorbents Calcined under Subatmospheric Conditions for the High-Temperature CO_2 Capture Process. *Ind. Eng. Chem. Res.* **46**, 35–42 (2007).

45. Reisman, A. Heterogeneous Equilibria in the System K2CO3-Na2CO3. *Journal of the American Chemical Society* **81**, 807–811 (1958).
46. Kim, S. M., Kierzkowska, A. M., Broda, M. & Müller, C. R. Sol-gel Synthesis of MgAl2O4-stabilized CaO for CO2 Capture. *Energy Procedia* **114**, 220–229 (2017).
47. Chen, J., Duan, L. & Sun, Z. Accurate Control of Cage-Like CaO Hollow Microspheres for Enhanced CO_2 Capture in Calcium Looping via a Template-Assisted Synthesis Approach. *Environ. Sci. Technol.* **53**, 2249–2259 (2019).
48. Naeem, M. A. *et al.* Optimization of the structural characteristics of CaO and its effective stabilization yield high-capacity CO2 sorbents. *Nat Commun* **9**, 2408 (2018).
49. Manovic, V. *et al.* Influence of calcination conditions on carrying capacity of CaO-based sorbent in CO2 looping cycles. *Fuel* **88**, 1893–1900 (2009).
50. MacDowell, N. *et al.* An overview of CO2 capture technologies. *Energy Environ. Sci.* **3**, 1645 (2010).
51. Kurlov, A., Armutlulu, A., Donat, F., Studart, A. R. & Müller, C. R. CaO-Based CO_2 Sorbents with a Hierarchical Porous Structure Made via Microfluidic Droplet Templating. *Ind. Eng. Chem. Res.* **59**, 7182–7188 (2020).
52. Broda, M. & Müller, C. R. Synthesis of Highly Effi cient, Ca-Based, Al 2 O 3 -Stabilized, Carbon Gel-Templated CO 2 Sorbents. *Advanced Materials* **24**, 3059–3064 (2012).
53. Su, C., Duan, L. & Anthony, E. J. CO2 capture and attrition performance of competitive eco-friendly calcium-based pellets in fluidized bed. *Greenhouse Gas Sci Technol.* **8**, 1124–1133 (2018).
54. Ma, X., Li, Y., Duan, L., Anthony, E. & Liu, H. CO2 capture performance of calcium-based synthetic sorbent with hollow core-shell structure under calcium looping conditions. *Applied Energy* **225**, 402–412 (2018).
55. Erans, M., Manovic, V. & Anthony, E. J. Calcium looping sorbents for CO2 capture. *Applied Energy* **180**, 722–742 (2016).

56. Janz, G. J. Molten carbonate electrolytes as acid-base solvent systems. *J. Chem. Educ.* **44**, 581 (1967).

57. Raissi, A. T. & Block, D. L. Hydrogen: Automotive fuel of the future. *IEEE Power and Energy Mag.* **2**, 40–45 (2004).